

TWO-STEP MULTI-ILLUMINANT COLOR CONSTANCY FOR OUTDOOR SCENES

Sang-Ho Lee, Sung-Min Woo, Ji-Hoon Choi, Jong-Ok Kim

School of Electrical Engineering Korea University, Seoul, Korea

Email : {franky_, wsm79, risty, jokim}@korea.ac.kr

ABSTRACT

This paper proposes a novel two-step multi-illuminant algorithm for color constancy in outdoor scenes. We adopt different color constancy approaches for both primary and secondary illuminations. In the first step, an input image is white-balanced entirely using the existing single-illuminant color constancy method. Next, we extract the secondary illumination region, which typically corresponds to a shaded region in outdoor scenes. Finally, the shaded region is corrected by the guidance of the Planckian locus theory. Experimental results show that the proposed algorithm can achieve much smaller angular error than conventional multi-illuminant methods while color artifact is alleviated.

Index Terms— RGB correction, multi-illuminant, two-step color constancy, outdoor scene

1. INTRODUCTION

Color constancy is the ability of human visual perception to recognize the intrinsic object color regardless of the illuminant color. Since the camera machine does not have the ability of human color constancy, it is necessary to endow it with such a capability as a post-processing.

Color constancy is a fundamentally under-constrained problem, and it is significantly difficult to correctly recover the color which humans actually perceive under a variety of multi-illuminant environments as commonly observed in indoor and outdoor scenes. In particular, outdoor illumination is different from indoor. The former is a combination of sky and sun lights while the latter is a mixture of indoor and outdoor illuminations. Due to this distinct feature, color constancy for multi-illuminant requires more complex processing, and also produces unnatural color corrections under specific scenes frequently. It would be more effective to perform white balance separately in both indoor and outdoor scenes. This motivates us to focus on white balance exclusive for outdoor.

Many consumer cameras that have been widely deployed in real world are typically equipped with color constancy capability for a single illuminant, and they show a poor performance of color reproduction under a multi-illuminant environment. Even though so many methods have been proposed for multi-illuminant, they may not be backward compatible to a single illumination. Thus, we propose a new approach which is easily scalable to multiple illuminants in outdoor scenes. The proposed method extends the existing color constancy methods to support multi-illuminant in a scalable way.

There have been recently proposed a number of color constancy methods for multi-illuminant scenes. Retinex theory by Land [1] is one of the early multi-illuminant color constancy methods and has been extended by several works [2], [3]. This theory assumes that depending on the location, the illumination changes smoothly but

the reflectance changes irregularly. In Ebner [4], local space average color (LSAC) is calculated by averaging adjacent pixels, and illumination is estimated by a weighted sum of the LSAC and the input image. This process is repeated more than 20,000 times until an illumination is converged to a fixed value. However, it makes the reproduced colors tend to be gray tone on the whole. Algorithms of [1] and [4] rely on the retinex theory, but it is not always satisfied in real worlds. For example, the colors of objects that are actually similar to each other look different for some uniform illumination scenes. This artifact is caused by the assumption of smoothly varying illumination. Meanwhile, Gijsenij [5] proposed a local illumination estimation algorithm by dividing an image into a number of clusters. An image is differently clustered every trial every trial, and accordingly, the results of illumination estimation are changed with trials. The method directly attempts to estimate two illuminants. In multi-illumination scenes, however, it is typically difficult to accurately estimate illuminants because illumination changes irregularly, depending on the location.

In this paper, we propose a novel two-step color constancy algorithm for outdoor scenes, assuming that sunlight and shadow cast as two illuminants. Unlike existing methods which remove the effects of multiple illuminants either locally or globally at the same time, the illumination of primary sunlight is first estimated and the reflectance is recovered in an entire image by utilizing existing methods for a single illuminant. Then we extract the secondary illumination region, which typically corresponds to shaded regions in outdoor scenes. Finally, the shaded region is corrected on a pixel basis by determining RGB correction ratio without explicit estimation of shade light. In this way, we adopt different color constancy approaches for both primary and secondary illuminations. This is a key difference, compared to conventional approaches. The illumination of shaded regions is not commonly from a light source directly in typical outdoor scenes, and its characteristics is similar to ambient light in a sense. Thus, it may be inappropriate to directly estimate shade light as a light source. In the proposed method, the pixel-by-pixel correction approach makes it possible to effectively solve the challenge for secondary shade light. In the case of directly estimating illumination, there may happens the color artifact (unnatural color change) at the border region between two illuminants due to the sudden change of the estimated illumination. Meanwhile, in the existing methods that do not estimate illuminants explicitly, the border artifact hardly occurs, but the accuracy of the illumination estimation is lowered even for primary illuminant as confirmed in the experimental result.

This paper is organized as follows. Section 2 describes the shaded region detection and color correction in the proposed algorithm. Section 3 shows the experimental results. Finally, Section 4 concludes the paper.

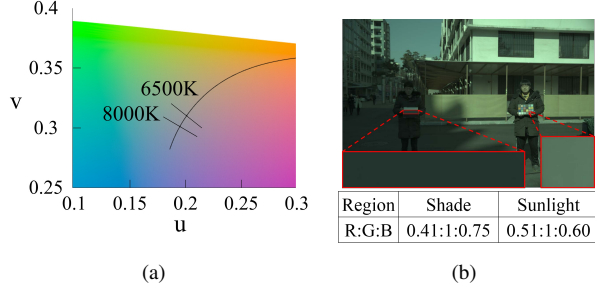


Fig. 1. (a) CIE 1960 uv color space. (b) the RGB ratio comparison of the shaded region with the sunlight. Note that the RGB ratio represents the relative ratio of R and B to the G channel.

2. TWO-STEP COLOR CONSTANCY FOR MULTIPLE ILLUMINATION

There have been developed so many color constancy methods for a single illumination. Even though those methods work well for a single illumination, they exhibit poor color reproduction for the secondary illumination in a multi-illumination scene. A couple of multi-illumination methods have been studied recently. But, it is still highly challenging to support diverse multi-illumination scenes including indoor and outdoor. For example, incorrect color reproduction can be widely affected in an entire image if primary illumination is estimated inaccurately. Also, the unnatural color change is visible at the border region between two different illuminations even if illuminations are well estimated.

In this paper, outdoor scenes, which are a combination of sunlight and shade light, are focused in particular because outdoor scenes actually appear frequently in the shooting environment. We propose a novel two-step approach. The primary goal of our work is to extend existing single-illuminant color constancy methods such that they could work well for multi-illuminant scenes. This is a very practical approach because many imaging devices have been already equipped with their own excellent single-illuminant techniques. Our work can make existing methods scalable to multiple illuminations.

2.1. Motivation

Fig. 1 (a) shows the CIE 1960 uv color space, where the curve is called the Planckian locus. It is known that natural illumination is located near the Planckian locus. For example, the color temperature of daylight corresponds to about 6500K while the color temperature of shade light is roughly over 8000K. We can see from Fig. 1 (b) that shade light tends to be a lower red ratio and a higher blue ratio than sunlight. Fig. 1 (a) indicates the relative color distribution according to its position in the CIE 1960 uv color space. Red becomes stronger toward the upper right direction while blue becomes stronger toward the opposite lower left in the color space. Since a shaded region is located at the lower left direction (near 8000K in Fig. 1 (a)), compared to a sunlight region, we can see that red is insufficient and blue is too strong. Fig. 1 (b) shows the representative result for the effects of the shade and sunlight on the colors of the image. The RGB ratios of the shaded and sunlight regions were actually calculated using the gray color of the color checker. A gray region is extracted from the color checker for both the shaded and sunlight regions. In the color checker, the RGB ratio is calculated relative to the G channel, and its values are specified in Fig. 1 (b). It can be observed from Fig. 1

(b) that shade light has a lower red ratio and a higher blue ratio than the sunlight. This implies that for ideal color constancy in a shaded region, red channel intensity should be increased while blue should be decreased. Guided by these observations, we propose color correction for the secondary shade illumination in the second step of the proposed method.

2.2. Shaded region detection

In a typical environment where two lights are mixed, there is no correlation between them, so it is difficult to separately partition two illumination regions. However, in the case of outdoor images with sunlight and shade light, the shaded region has a relatively low brightness value compared to the sunlight, so there is a high correlation between illumination and brightness. Therefore, the brightness (or pixel intensity) of the image can be effectively used to distinguish two illumination regions of sunlight and shade.

In the outdoor image, sunlight region is separated from shade, based on thresholding brightness value. It is assumed that a shaded region is less than a certain percentage of maximum brightness level in the image. Without setting the threshold to a fixed brightness value, the threshold is put on the percentage (denoted by c_t in (1)) of maximum brightness level. Thus, the actual threshold varies with maximum brightness value of the image as follows.

$$\mathbf{T} = c_t \times \mathbf{I}_{\max} \quad (1)$$

where \mathbf{I}_{\max} is the maximum intensity in the image, \mathbf{T} is a threshold value, and c_t is a parameter to determine the threshold for the shaded region. It is very challenging to exactly extract a shaded region in real world images, and the performance of the thresholding based method may be sensitive by the parameter configuration. However, the proposed method performs color correction smoothly at the border region and does not require accurate boundary between two illuminations. The details are described in next subsection.

2.3. Correction in the shaded region

Under multi-illuminant of sunlight and shade, the shaded region is required to be further white-balanced even though the sunlight one has been already corrected with a single illumination estimation. In this subsection, we propose a method to further correct the R and B channels in the RGB color space. The ranges of R and B channel values are first determined based on the G channel in the shaded region in order to obtain R and B correction ratios. The ranges of R and B can be determined as follows.

$$\mathbf{S}_r = \{\mathbf{i} | c_r \times \mathbf{G}_i < \mathbf{R}_i < \mathbf{G}_i\}, \quad \mathbf{R}_m^r = \frac{1}{|\mathbf{S}_r|} \sum_{i \in \mathbf{S}_r} \mathbf{R}_i, \quad \mathbf{G}_m^r = \frac{1}{|\mathbf{S}_r|} \sum_{i \in \mathbf{S}_r} \mathbf{G}_i \quad (2)$$

$$\mathbf{S}_b = \{\mathbf{i} | \mathbf{G}_i < \mathbf{B}_i < c_b \times \mathbf{G}_i\}, \quad \mathbf{G}_m^b = \frac{1}{|\mathbf{S}_b|} \sum_{i \in \mathbf{S}_b} \mathbf{G}_i, \quad \mathbf{B}_m^b = \frac{1}{|\mathbf{S}_b|} \sum_{i \in \mathbf{S}_b} \mathbf{B}_i \quad (3)$$

where \mathbf{i} is the index of a pixel, and \mathbf{R}_i , \mathbf{G}_i , \mathbf{B}_i are the R, G, B channel values of a pixel index \mathbf{i} , respectively. As shown in Fig. 1 (a), colors in the shaded region are affected by the illuminant with color temperature higher than sunlight. This means that for shade light colors, the ratio of red to green is lower while the ratio of blue to green is higher, when compared to the sunlight. Under these assumptions, the range of the R channel, \mathbf{S}_r is chosen such that it is smaller than the G channel. Note that a parameter, c_r is multiplied

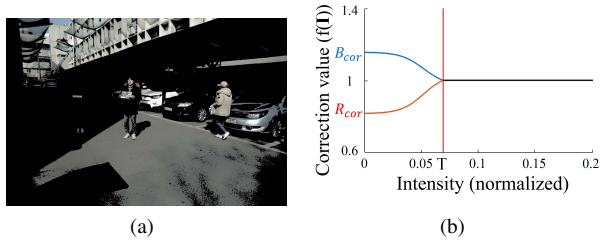


Fig. 2. (a) Estimated shaded region using thresholding (pixels whose intensity is below the threshold (T in (1)) are marked in black) (b) The curve of correction values for both R and B channels.

in order to exclude too small values. The range of the B channel, S_b is also chosen, similar to S_r . The ratio of blue to green is higher, so the B channel should be larger than green. In order to exclude too large values, the upper value of B is limited by multiplying c_b . After determining the ranges of R and B, we calculate the average values of the R and B pixels belonging to the corresponding range in the shaded region. Finally, the correction values of the R and B channels are calculated as

$$R_{cor} = \frac{R_m^r}{G_m^r}, \quad B_{cor} = \frac{B_m^b}{G_m^b}. \quad (4)$$

When shaded regions are extracted using the thresholding method in previous subsection its extraction may be inaccurate. If the correction values R_{cor} and B_{cor} obtained from (4) are uniformly constant for all pixels in the shaded region, color artifact can happen near the border between sunlight and shade. In order to reduce this color artifact, the correction value is determined to vary smoothly on the border region as shown in Fig. 2 (c). The equation of the correction graph is as follows.

$$f(I) = \begin{cases} \frac{C_{cor}-1}{1+\exp\{p(I-\frac{3}{4}T)\}} + 1 - \frac{C_{cor}-1}{1+\exp\{p(\frac{1}{4}T)\}}, & I \leq T \\ 1, & I > T \end{cases} \quad (5)$$

where C is an R or B channel ($C \in \{R, B\}$) and p is a curvature parameter.

The correction values of the R and B channels are modeled by gradual decreasing and increasing curves from the border, respectively. As illustrated in Fig. 2 (c), the correction value is fixed to 1 for the sunlight region where the normalized intensity is larger than the threshold. This means that the pixels of the sunlight region is kept unchanged. The correction value gradually increases or decreases according to channel, but both correction values are close to 1 as the normalized intensity approaches the threshold (i.e., the border line between sunlight and shade in the image). This correction design has advantage in that we do not need to process the sunlight and shaded regions separately.

3. EXPERIMENTAL RESULTS

In existing color constancy data sets in academia, there are not so many outdoor images, and furthermore, there is no ground truth due to its difficulty to acquire. Thus, we produced 30 test images ourselves which were taken with a Canon EOS 5D Mark III camera on a clear day or a slightly cloudy day. All test images include the color checker in the scene in order to produce a ground truth image. The proposed method can extend any single illumination methods to multi-illuminant environments. In the experiment, the parameters

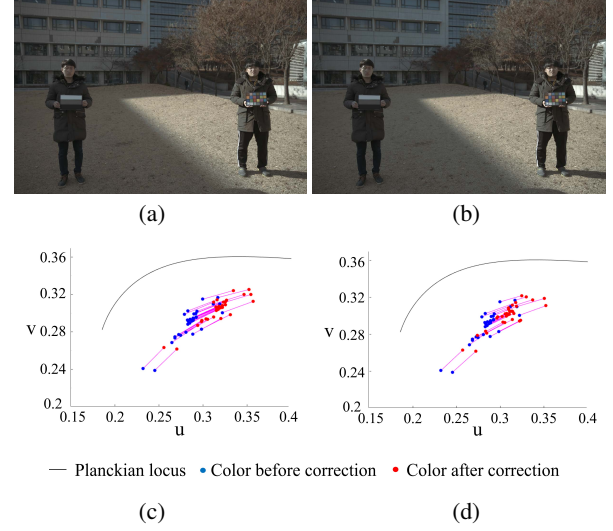


Fig. 3. (a) the ground truth (color correction with the gray color of the color checker in the image) (b) the proposed method (c) and (d) show the direction of color correction by (a) and (b), respectively.

were set to $c_t = 0.08$ in (1), $c_r = 1.6$ in (2), $c_b = 1 / 1.6$ in (3), and $p = 100$ in (5).

First, we verify the performance of the proposed algorithm to white-balance the shaded region properly. Since the illuminant of the target outdoor image is a natural light, it dynamically changes with time, so it is difficult to obtain a ground truth image for comparison. The test image is white-balanced with the gray color of the color checker in the shaded region of the image, and the resulting image is regarded as a ground truth. Fig. 3 (c) and (d) show how the color of each pixel changes by the proposed method. The color change is denoted by a vector notation where the starting and terminal points represent the input color before color constancy and the corrected one after, respectively. The vectors move toward the direction of the low color temperature on the Planckian locus on the whole. If the proposed method (Fig. 3 (d)) is compared to the ground truth (Fig. 3 (c)), the directions of the vectors are similar to each other. This means that the proposed method can perform color constancy, in a similar way to the ground truth.

As shown in Fig. 2 (b), the amount of correction decreases, approaching the threshold closely. In other words, the proposed method can smoothly control the extent of color correction in the vicinity of the border. It is expected that the border region is actually affected by both lights simultaneously. It is highly challenging to correctly white-balance in this illuminant-mixture region. As shown in Fig. 3 (b), the visual color quality is very natural at the border region for the proposed method.

Next, the proposed method is compared with the conventional color constancy methods for multi-illuminant. For the case of the grey-edge (color constancy method for a single-illuminant) as shown in Fig. 4 (a), the shaded region is compensated by incorrect illumination. Thus, the border artifact is clearly outstanding due to its distinct color reproduction. Note that Fig. 4 (a) corresponds to the result of the first step in the proposed method. Fig. 4 (b) shows the result when the grey-edge is separately applied to both sunlight and shaded regions, which are partitioned by the proposed thresholding method. The result of [6] is shown in Fig. 4 (c) where it can be observed that

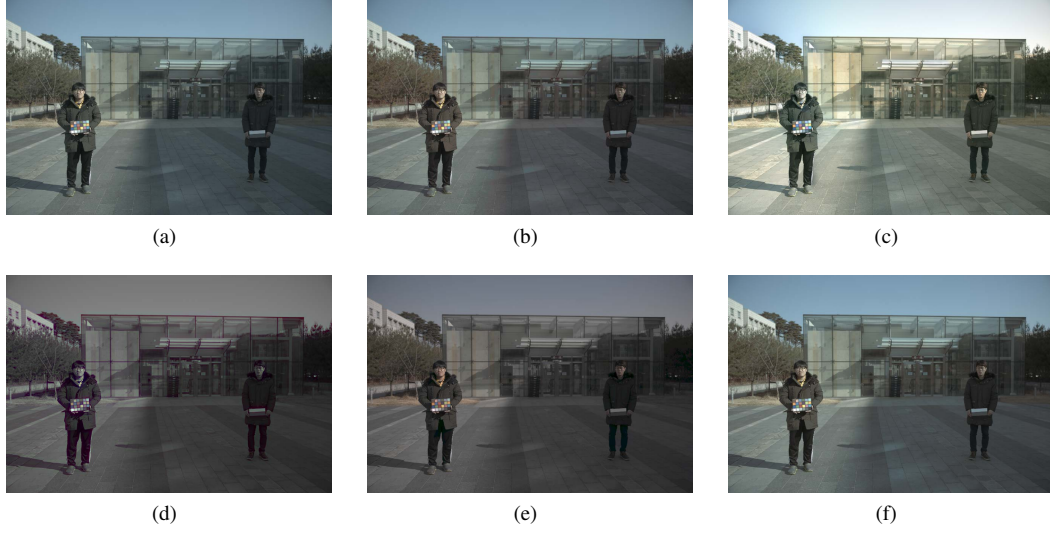


Fig. 4. The result images of color constancy algorithms. (a) grey-edge (b) grey-edge (applied to sunlight and shaded regions separately) (c) Retinex [6] (d) Ebner's algorithm [4] (e) Gijsenij's algorithm [5] (f) the proposed algorithm

Table 1. Angular error in sunlight region

Method	Mean	Median	Best-25%
Retinex [6]	10.9°	11.4°	7.8°
Ebner [4]	4.4°	4.1°	3.0°
Gijsenij [5]	18.9°	6.5°	1.4°
Proposed	2.4°	2.1°	0.9°

Table 2. Angular error in shaded region

Method	Mean	Median	Best-25%
Retinex [6]	8.4°	7.9°	4.5°
Ebner [4]	4.2°	4.0°	3.4°
Gijsenij [5]	20.2°	12.6°	3.1°
Proposed	3.5°	3.3°	0.8°

the color of the face skin changes. We can see that the retinex theory is not satisfied for the scene of Fig. 4 (c). For Ebner's algorithm [4] in Fig. 4 (d), the illuminant is estimated on a pixel basis, and the corrected image appears to be a gray tone as a whole. As shown in Fig. 4 (e), in Gijsenij's algorithm [5] the color of the primary sunlight region is not recovered correctly due to inaccurate illumination estimation. As shown in Fig. 4 (f), the proposed method has less color artifacts caused by incorrect illumination estimation because it does not estimate the secondary illuminant directly. Note that the primary illuminant can be estimated well with the existing grey-edge method as confirmed in Fig. 4 (a). But, even though the grey-edge is applied to the shade region only, it fails to correctly reproduce the colors in the shaded region as confirmed in Fig. 4 (b). This result shows the difficulty of estimating the secondary shade illumination. The proposed method utilizes existing methods for the estimation of the primary illumination. The secondary illumination is not estimated explicitly, and instead, RGB values are corrected in order to remove its effect. Objective evaluation results are compared in Table 1 and Table 2. The proposed method achieves much smaller angular error than conventional methods for both sunlight and shaded regions. Finally, the proposed method is actually integrated into the consumer smartphone (LG G5) in order to verify its easy implementation to practical devices. Fig. 5 (a) shows the result of LG G5 color constancy (a single-illuminant method), while Fig. 5 (b) illustrates the result of LG G5 + the proposed. It is shown that the proposed method can further enhance the color reproduction by being combined with the existing practical single-illuminant method.



Fig. 5. The results of color constancy (a) LG G5 only (b) the combination of the proposed with LG G5

4. CONCLUSION

In this paper, we proposed a novel two-step color constancy method for multi-illuminant outdoor scenes. In the first step, an input image is white-balanced with single-illuminant methods. Next, the region of the secondary illuminant (or shaded region) is extracted using the intensity thresholding method. Then, the correction ratios of R and B channels are determined for the shaded region, guided by the Planckian locus theory. Experimental results show that the proposed two-step method can achieve much smaller angular error than conventional multi-illuminant methods. Also, it shows the natural transition of the colors at the border region. In addition, it was demonstrated that the proposed method can extend any conventional single-illuminant methods to support multi-illuminant. Thus, it can be easily implemented in existing devices with the capability of a single-illuminant color constancy.

5. REFERENCES

- [1] Edwin H Land and John J McCann, "Lightness and retinex theory," *Josa*, vol. 61, no. 1, pp. 1–11, 1971.
- [2] Zia-ur Rahman, Daniel J Jobson, and Glenn A Woodell, "Multiscale retinex for color image enhancement," in *Image Processing, 1996. Proceedings., International Conference on.* IEEE, 1996, vol. 3, pp. 1003–1006.
- [3] Daniel J Jobson, Zia-ur Rahman, and Glenn A Woodell, "A multiscale retinex for bridging the gap between color images and the human observation of scenes," *IEEE Transactions on Image processing*, vol. 6, no. 7, pp. 965–976, 1997.
- [4] Marc Ebner, "Color constancy using local color shifts," in *European Conference on Computer Vision*. Springer, 2004, pp. 276–287.
- [5] Arjan Gijsenij, Rui Lu, and Theo Gevers, "Color constancy for multiple light sources," *IEEE Transactions on Image Processing*, vol. 21, no. 2, pp. 697–707, 2012.
- [6] Brian Funt, Florian Ciurea, and John McCann, "Retinex in matlab," *Journal of electronic imaging*, vol. 13, no. 1, pp. 48–57, 2004.